

Article

Direct Method to Design Solar Photovoltaics to Reduce Energy Consumption of Aeration Tanks in Wastewater Treatment Plants

Enrico Zacchei ^{1,2,*}  and Antonio Colacicco ³¹ Itecons, 3030-289 Coimbra, Portugal² University of Coimbra, CERIS, 3004-531 Coimbra, Portugal³ Environmental Engineer-Freelancer, Luigi Pernier Avenue, 00124 Rome, Italy; antonio_colacicco@hotmail.it

* Correspondence: enricozacchei@gmail.com

Abstract: Photovoltaic (PV) energy systems are considered good renewable energy technologies due to their high production of clean energy. This paper combines a PV system with wastewater treatment plants (WWTPs), which are usually designed separately. For this, a recent methodology was adopted, which provides direct steps to estimate the peak powers of PV plants (PVPs) by using the airflow of blowers. The goal was to reduce the energy consumption of aeration tanks in WWTPs. Analytical equations and parameters based on the air temperature, solar irradiation, biological kinetic, dissolved oxygen, and mechanical oxygenation are adopted. The key parameter in this methodology is the air temperature variation that represents an approximated temperature in the WWTP's oxidation tanks. It is shown, through the analysis of small WWTPs, that since the temperature changes for each season, there is a peak in the function of the quantity of oxidation, which is high in the summer season. Further, the curve trends of temperature for WWTPs are similar to PVPs. Therefore, it could be possible to design the PV system with the WWTPs well. The results show that the air temperature curves increase in a directly proportional way with the consumption of energy from oxidation blowers; this could induce a more conservative PVP design. Furthermore, the results show that the mean trend of the energy consumption of the analyzed aeration systems reaches about 8.0% at a temperature of 20–25 °C, covering a good part of the oxidation tank consumption.

Keywords: auto-consumption systems; clean energy; oxidation tanks; PVP; WWTP



Citation: Zacchei, E.; Colacicco, A. Direct Method to Design Solar Photovoltaics to Reduce Energy Consumption of Aeration Tanks in Wastewater Treatment Plants. *Infrastructures* **2022**, *7*, 79. <https://doi.org/10.3390/infrastructures7060079>

Academic Editors: Susana Lagüela López and GM Shafiullah

Received: 6 April 2022

Accepted: 2 June 2022

Published: 6 June 2022

Publisher's Note: MDPI stays neutral with regard to jurisdictional claims in published maps and institutional affiliations.



Copyright: © 2022 by the authors. Licensee MDPI, Basel, Switzerland. This article is an open access article distributed under the terms and conditions of the Creative Commons Attribution (CC BY) license (<https://creativecommons.org/licenses/by/4.0/>).

1. Introduction

Photovoltaic (PVPs) plants are considered good renewable energy technologies since they have a high potential for clean energy productivities [1]. They have various environmental advantages, for instance, in producing low fossil-fuel and CO₂ emissions. Moreover, PVPs are based on auto-consumption due to the free input energy.

This paper aims to develop a smart method for designing PVs by optimizing the auto-consumption of oxidation tanks in wastewater treatment plants (WWTPs). For this, the key design parameters are the air and wastewater temperatures and their correlations. Some parameters that consider the bacteria respiration have also been accounted for in accordance with innovative projects [2,3].

PVPs are treated in the literature at the level of forecasting power generations, where several time series prediction statistical methods and algorithms on artificial intelligence are introduced, investigating the effect of prediction time horizon variation [1] and of the design in extreme conditions, where mathematical models to predict the energy generation of PVPs in hot and humid climatic condition are studied [4]. In [1,4], some parameters were studied that impact the electrical power generation, e.g., the type of solar cells and their conditions, electrical circuits of modules, solar incidence angle, and weather conditions.

In [5], a state-of-the-art PV solar energy generator has been made, showing the ways of obtaining the energy, its advantages and disadvantages, applications, current market, costs,

and technologies. Here, the possible applications are shown, e.g., for telecommunications, water pumping, agriculture, water heating, grain drying, water desalination, and space vehicles and satellites.

WWTPs have been treated by considering the aeration energy consumption, where a fuzzy logic supervisory control system for optimizing nitrogen removal has been developed [6], the influence of seasonal temperature fluctuations on raw domestic wastewater composition and collected sludge filterability [7], and the balance of the micropollutant flows, where a simple balancing method using passive samplers over a period has been tested to determine the elimination rates of several common micropollutants of household and industrial sources in full-scale WWTPs of different performances [8].

In [9], a complete review has been shown to provide a technical contribution to the regulations as well as to support stakeholders by recommending possible advanced treatment options, in particular, the removal of contaminants of emerging concern and antibiotics, antibiotic-resistant bacteria, and antibiotic resistance genes.

In [10], some strategies to achieve environmental sustainability for wastewater treatments are presented; in particular, it examines how environmental technology contributes to wastewater improvement in several countries. Annualized information was used and collected from various official sources of information and subsequently processed with various econometric approaches.

As mentioned, this paper combines PVP with a WWTP since solar PV has a great generation potential in WWTPs. It is known that technical, economic, and socio-political factors influence the decision to adopt solar PVs in WWTPs as treated in [11,12].

Some papers that combine PVs with WWTPs have been published. In [13], a direct connection of PV modules to the electrochemical reactor was carried out to reduce the non-renewable primary energy consumption; for this, a solar PV electro-oxidation process for WWTP was modeled; in [14], both plants are combined with each other to design floating PVs installed on, e.g., natural lakes, dams reservoirs, and offshore areas, where a simple and economic design solution in South Australia with optimal orientation and distance among rows was suggested; in [15], where a wastewater-to-hydrogen processor was proposed to maximize the hydrogen and minimize the energy consumption. In [16], the control and planning for energy durations, where the feasibility of using solar PV cells and a battery system as a renewable energy source for driven electrochemical WWTPs were studied; whereas in [17], the feasibility and utility of using an electro-oxidation system directly powered by a PV array for the treatment of wastewater was demonstrated.

More recent papers have carried out a quantitative analysis of the solar energy generated from WWTPs where specific 105 Californian WWTPs were examined, of which 41 installed a solar PV system [18]. In [19], it was shown that the synergy of small and medium WWTPs with PV is of great interest from an energetic/environmental/economic point of view; it was stated that “this synergy is worth exploring and implementing on a large scale for all new WWTP”. Therefore, more studies are necessary.

Moreover, in [20], electric energies from PV modules were used to remove aniline in wastewater, showing that this process is feasible, and aniline can be removed in a safer and lower-cost way. In [21], it was highlighted that small and insular communities are sometimes not served by an efficient WWTP, and this was a hazard for both the environment and public health. For this, it was shown that a PV system covers the electricity needs of the apparatus. Thus no external electricity source should be necessary for its use. This coupling could be used to minimize the community’s costs.

The motivation of this research is based on some critical analyses published in previous studies [22,23], which should justify the two main hypotheses for this work: (i) the oxidation tanks consume ~30.0% of the total cost of the energy of a WWTP. Thus the use of a PV could cover part of this consumption in a clean way; (ii) for a small treatment plant, the energy consumption is high in the function of the oxygenation in aeration blowers where a PV could be installed.

Further, through the analysis of the Zurich WWTP, in [24], it is shown that the temperature of wastewater in the entrance changes for each season. For a small WWTP, a peak of energy consumption in the summer was verified since when the temperature of the wastewater increases the oxygen consumption, thus the aeration blowers need to work more.

Therefore, through critical analyses, some preliminary data have been collected that, with the relations and parameters on the oxygen consumption and temperature, provide several materials to be used in this work (Section 2.1). Section 2.2 shows the model, where its goal is to provide some analytical relations to design PVPs to reduce the energy consumption of WWTPs since they represent an important part of the “anthropic water cycle” [12]. Finally, in Section 3, analyses and results have been presented in terms of energy consumption of blower’s aeration systems with respect to PV plants to evaluate the good and/or optimum performance of the system.

This work could help the sector make decisions over PV investments, especially regarding wastewater utilities, which ultimately lead to more sustainable management practices. Thus, we encourage a further contribution to promoting the integration of renewable energy sources as PVPs, together with WWTPs and their sectors.

This purpose is consistent with goal 7 of the 2030 Agenda [25] in order to “ensure access to affordable, reliable, sustainable and modern energy for all”.

2. Materials and Methods

2.1. Materials

2.1.1. Reference Data

The electricity consumption of an “anthropic water cycle”, considering the final uses (e.g., agricultural, civil, and industrial uses), ranges between 1.0 and 8.0 kWh/m³. This consumption of energy includes a percentage, without including the final uses, between 1.0% and 5.0% of the national electricity requirements and between 5% and 20%, including the final uses [22].

The flowchart in Figure 1 shows the process diagram of the water management cycle (water source → water body) from withdrawal (i.e., pumping and transport) to the wastewater disposal, where the water body is re-introduced in accordance with the European directive [26]. It is shown that the “wastewater treatment” phase (yellow box in Figure 1) allows the closing/opening and continuation of this cycle.

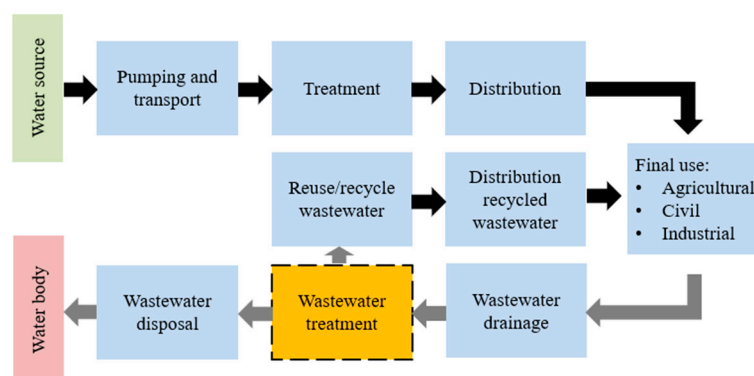


Figure 1. Water management cycle: process diagram (adapted from [22]).

As already mentioned, in urban WWTPs, it is estimated that ~30% of the costs of the management are attributed to energy consumption, even if ~50% can include additional costs of the other treatments, as shown in [22,23].

The electricity consumption of a WWTP with anaerobic sludge digestion is between 0.40 and 0.70 kWh/month in function of the type/size of the studied plant. In general, WWTPs have an electricity consumption between 10 and 40 kWh/PE per year (PE is the population equivalent estimated as 1 PE ≈ 60 gBOD₅/d [8], where BOD₅ is the biochemical

oxygen demand during the day, d), whereas in a WWTP, with digestion of an aerobic-type, the electricity consumption can reach values of 40–70 kWh/PE per year due to the lack of energy to be recovered [23].

The BOD₅ parameter includes the biodegradable portion of the organic substances with respect to the chemical oxygen demand (COD) parameter, which measures the global oxidation of (in)organic substances.

The biological oxidation regards the highest percentage of total consumption (e.g., 50–65%), then there are the treatment lines of the sludge, which can reach a consumption of 20%, and, finally, there is the pumping phase, using ~15% [23].

In the WWTPs of urban sludges, a great part of the electricity is used in the oxidation tanks by the aeration process. The percentage incidence of the consumption of the energy, in the function of the operation costs, as well as maintenance costs, are shown in [23], with the following weight: 50% energy, 21% management, 13% chemical, 11% maintenance, 5% others.

In [23], it is shown that the distribution of the electricity in the various steps of traditional WWTPs, in particular, the oxygen aeration in tanks, is the greatest with a value of 55.6%, whereas the lowest value refers to pre-treatment of the wastewater process with a value of 0.4%. Moreover, by analyzing 253 WWTPs, an acceptable agreement between the total consumption of the energy of WWTPs and the volume of sewage flows was shown. In the same way, the impact of the large plants, which have low energy consumption (expressed in m³) of treated sewages and removed organic substances (in kg), has been highlighted.

Finally, an example of the specific consumption per kg of COD removed (expressed in kWh/kgCOD_{rem}) has been shown, which identifies the quality of the water by the variation of treatment classes for WWTPs. For a potential class < 2000 PE corresponds to a mean value of 3.21 kWh/kgCOD_{rem}, whereas for >100,000 PE, we have 0.85 kWh/kgCOD_{rem}.

All these data represent the input parameters that have incentivized this study.

2.1.2. Oxygen and Temperature Role

In the oxidation tanks, to activate the reactions of biological substances, the presence of dissolved oxygens (DOs) is necessary; thus, its continuous creation to equilibrate the consumption of the carbon-oxidant bacteria respiration is also necessary [2,9,27]. DO is a parameter that allows the control of the biological process in relation to the energy reduction [6,28]; also, the biological oxidation processes are correlated to the temperature, T.

The biological reactions can increase with a temperature between 0 and 40 °C with an estimated optimum T between 25 and 35 °C. However, in the aeration tanks, the latter temperatures are rarely achieved. With a temperature T < 5 °C, the biological activity can strongly decrease [29].

The respiration of the bacteria is quantified by two different coefficients: active breathing, *a* (Equation (1)), and endogenous respiration, *c_T* (Equation (2)).

The *a*-coefficient is correlated to the oxidative reactions as well as synthesis reactions where the microorganisms take energy by their own metabolism and by the creation of new cell synthesis. Further, this coefficient represents the consumption of oxygen for the destruction of the organic substances, which is proportional to the removed substrate of carbonaceous [30].

This *a*-coefficient varies with respect to the WWTP used, and it can be evaluated by [30]:

$$a = \frac{0.65 \times \text{kg}_{\text{O}_2}}{\text{kg}_{\text{BOD}_5}} \quad (1)$$

where kg_{O₂} is the mass of the consumption of oxygen (O₂), and kg_{BOD₅} is the mass of the BOD₅ concentration. Both parameters are correlated with each other through the volume of the oxidation reactor, V_{oxi}, by kg_{BOD₅} = V_{oxi} × BOD₅.

The other coefficient, i.e., endogenous respiration, is related to the use of the available substrate for critical temperature and demolition of bacteria cells. In this sense, it regards

the metabolism of the bacteria. This endogenous respiration coefficient, c_T , can be described by [30,31]:

$$c_T = c_{20} \times 1.084^{T-20} = \left(\frac{0.13 \times \text{kg}_{\text{O}_2}}{\text{kg}_{\text{VSS}} \times \text{d}} \right) \times 1.084^{T-20} \quad (2)$$

where c_{20} refers to a c value of 20 °C (i.e., $c_T = 20 \rightarrow c_{20}$), and kg_{VSS} is the mass of volatile suspended solids (VSSs).

Therefore, the oxygen consumption can be expressed by [6,30]:

$$R_{\text{O}_2} = \frac{a \times \text{kg}_{\text{BOD}_5}}{\text{d}} + \frac{c_T \times \text{kg}_{\text{Biomass}}}{\text{d}} \quad (3)$$

where $\text{kg}_{\text{Biomass}}$ is the biomass ($= V_{\text{oxi}} \times \text{VSS}$; here approximated by $\text{kg}_{\text{Biomass}} \approx \text{VSS}$ [12]).

If there are no relevant variations of the kg_{BOD_5} during a season, the requirement of oxygen mainly varies due to the function of the T increasing due to Equation (2). Furthermore, in the wastewater, the oxygen concentration depends on Henry's law, which correlates the concentration of O_2 present in the liquid phase with respect to its concentration present in the gas phase [32]. In this study, this correlation indicates that the amount of DO is inversely proportional to the increase in the wastewater temperature. Therefore, to maintain an acceptable aerobic degradation of kg_{BOD_5} with an increasing wastewater T , in the oxygenation tanks, some oxygen "surplus" must be supplied. This implies that the aerator systems could work hard during the hot months to guarantee a sufficient concentration of DO [6,29].

In [7,29], the fluctuation of the wastewater T as a function of time is shown. In [26], the air temperature curve where it is evident that the curves of the high/low temperatures of the wastewater vary, with a maximum value in summer months (i.e., July in the Mediterranean area) is also plotted. These fluctuations of the curves refer to a small plant since they do not fluctuate (i.e., they are quasi-constant) in large plants.

An important phenomenon regards the overlapping of the wastewater temperature curves (high and low) with the curve that shows the maximum air temperature. This overlap happens in small WWTPs, because of the seasonality, which is directly correlated with the irradiation/temperature. Therefore, the adoption of the air temperature values for the design could provide a good estimation regarding the thermal trend of the wastewater overdesign, in favor of safety, the PVPs.

Finally, some aspects should also be mentioned to indicate the increase in the temperature of the wastewater (influent) flow in hot periods, which are associated with high proliferation of organic substances in WWTPs with small and/or medium size. This increase can amplify the total consumption of energy, mainly involving the aeration systems for producing oxygen.

These aspects regard the energy (see two hypotheses in Section 1), chemical–physical, and biological factors. Regarding the chemical–physical factors in the wastewater: (1) the temperature oscillates due to its seasonality, and due to the wastewater flow rate; (2) the increase of the T reduces the solubility of the oxygen. The biological factors include (3) the increasing of the wastewater flow rate and the oxygen requirement of organic substances for the kinetic digestions.

Small WWTPs have greater power consumption than large plants, making them more sensitive to increases in energy cost [33]. Therefore, it is important for small plants to find alternative energy sources to increase resilience to energy cost fluctuations. Solar PV represents a suitable source of energy for small WWTPs for two main reasons: the lack of biogas recovery opportunities and land availability [18].

Table 1 shows the parameters used to carry out the analyses. Some parameters have already been explained, whereas other ones will be explained in Section 2.2.

Table 1. Data used for the analysis.

| Parameter | Value |
|--|--|
| Active breathing coefficient, a | 0.65 (Equation (1)) ^a |
| Biochemical oxygen demand, BOD_5 | 0.8 kg _{BOD5} ^b |
| Endogenous respiration coefficient, c_T | 0.09–0.19 (Equation (2)) ^c |
| Volatile suspended solids, VSS | 4.0 kgVSS [12] |
| Correction factor, α | 0.80 [30] |
| Aerators fouling factor, F | 0.90 [12] |
| Correction factor, β | 1.0 [30] |
| Standard aeration efficiency, SAE_{20° | 1.55–3.0 kgO ₂ /kWh [34] ^d |

^a Assuming kgO₂ = kg_{BOD5}. ^b The value is correlated to the sludge loading rate (SLR) by: $SLR = BOD_5/VSS = 0.20$ [8,12].

^c With $c_{20} = 0.13$ and $T = 15\text{--}25^\circ\text{C}$. ^d For clean water at 20°C , pressure of 101.32 kPa, and DO = 0 mg/L. The SAE value depends on the adopted aeration system.

2.2. Methodology

For estimating the maximum consumption of energy of a selected aeration system, direct analytical equations, recently introduced in [12], have been used. These equations should verify the energy consumption variations of a certain aeration system regarding the oxygen requirements and wastewater temperature in oxidation tanks.

Considering the relations already mentioned in Section 2.1.2, i.e., $kg_{Biomass} = V_{oxi} \times VSS$ and $kg_{BOD5} = V_{oxi} \times BOD_5$, Equation (3), by multiplying for d and dividing for V_{oxi} , describes the incremental parameter of R_{O2} , I_{RO2} , which estimates the increasing of R_{O2} with respect the standard temperature T (i.e., $T = 20^\circ\text{C}$) in the wastewater. It is defined, as a percentage (%), as:

$$I_{RO2} = \frac{[(a \times BOD_5) + (c_T \times VSS)] - [(a \times BOD_5) + (c_{20} \times VSS)]}{[(a \times BOD_5) + (c_{20} \times VSS)]} \quad (4)$$

An aeration blower should be defined by the oxygen transfer capacity, i.e., the oxygen transfer rate (OTR):

$$OTR = SOTR \left(\alpha \times 1.024^{(T-20)} \times \frac{\beta(C_s - C_L)}{C_s} \times F \right) \quad \text{with } SOTR = \left(1.024^{(T-20)} \times \alpha \times F \right) \quad (5)$$

where C_L is the service oxygen concentration and C_s is the saturated oxygen concentration. Both concentrations are expressed in mg/L, and here, they are assumed to be $C_s = C_L$, neglecting the dynamic component of gas concentration. α , β , and F (i.e., aerator fouling factors) are constants. SOTR is the standard-OTR, which refers to the oxygen measurements in the clean water under standard pressures and temperatures. OTR is expressed in kgO₂/h.

From Equation (5), the incremental parameter of SOTR, I_{SOTR} (in %), is:

$$I_{SOTR} = \frac{(1.024^{(T-20)} \times \alpha \times F) - (\alpha \times F)}{(\alpha \times F)} \quad (6)$$

For measuring the variation of the SAE, I_{SAE} , with respect 20°C (i.e., SAE_{20}), and by considering Equation (6), Equation (7), expressed in kgO₂/kWh, is used:

$$I_{SAE} = SAE_{20} + (SAE_{20} \times I_{SOTR}) \quad (7)$$

Finally, to correlate I_{SAE} with the I_{RO2} (Equation (4)) Equation (8), in %, is used:

$$I_{PRO2} = \frac{1}{I_{SAE}} \times I_{RO2} \quad (8)$$

Equation (8) provides the main output that allows the energy consumption values for different aeration blowers adopted in the oxidation tanks to be plotted.

The general methodology can be described step-by-step as follows: (i) collection of data by database, the literature, and Equations (1)–(3) (see Table 1); (ii) plotting the average monthly energy production curves, E_m (see Section 3); (iii) estimation of I_{RO2} curves by the proposed equation, Equation (8), for 5 aeration systems; (iv) defining the performances of the coupled system (see Section 3).

3. Analyses and Results

The analyses consist of developing the above-mentioned equations for a general case and then for a specific example. The correlation key of the analyses regards the fact that the energy consumption of the aeration blowers should measure the whole energy consumption of the WWTP. This correlation represents an important issue for the whole system in order to maintain the equilibrium of the energy.

In Equations (4) and (6), the following (some) values have been calculated for wastewater $T = \{15, 20, 25\}$ °C: $I_{RO2} = \{-16.6, 0, 24.8\}\%$, and $I_{SOTR} = \{11.2, 0, -12.6\}\%$. Thus, the I_{SAE} (Equation (7)) and I_{PRO2} (Equation (8)) values are obtained for five aeration systems: (1) large bubble ventilation; (2) surface aerators with low speed; (3) surface turbines with downward flow; (4) superficial brushes; and (5) submerged turbines with injector.

Figure 2 shows the results of I_{PRO2} with respect to the wastewater T in the oxidation tanks. These curves are calibrated at $T = 20$ °C (middle point), which represents, as already mentioned, the standard conditions.

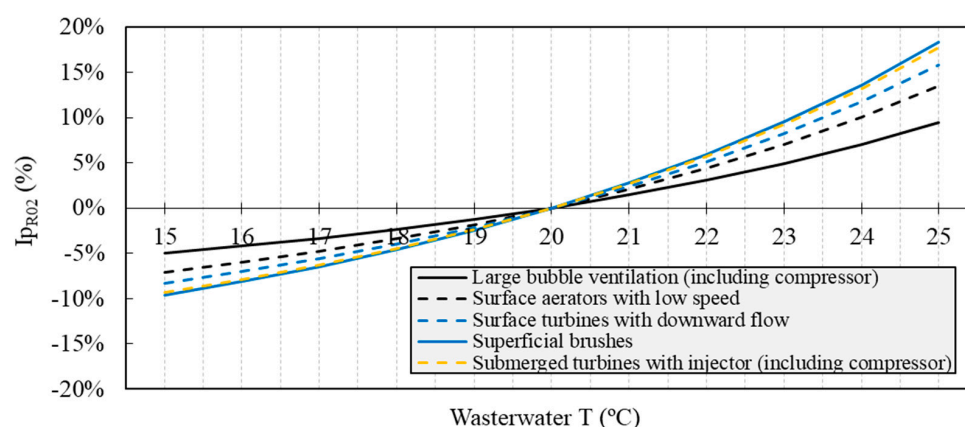


Figure 2. I_{PRO2} values as a function of wastewater T for five aeration systems.

The curves in Figure 2 allow the quantification of not only the aerator technology that can be classified as most energy-efficient but also the increasing of the seasonal consumption of energy of the considered aerator, independently of the influent flow rate of BOD_5 .

It is shown that the trend of the I_{PRO2} curves for the five aeration systems ranges between -10% and 18% for 15 – 25 °C. The “superficial brushes” (blue solid line) systems represent the technologies’s more energy intensiveness.

The “large bubble ventilation” (black solid line) is less energy-intensive; in fact, the presence of the bubbles in an aeration system is correlated to the energy generation; in particular, the dimension of the air bubbles affects the airflow and its velocity, as treated in [31].

Wastewater temperature mainly depends on the external air temperature and seasonality; therefore, this temperature could be approximated to the air temperature, as shown in [12]. The idea of using the air temperature curve should be in favor of safety since this curve would overestimate the PV system in terms of power outcomes covering the peaks of energy demands. In fact, in [29], it is shown that between ~ 8 and 20 °C, the external air temperature curve is higher than the high wastewater temperature curve.

To validate the methodology and the results shown in Figure 2, an example has been carried out. To design the peak powers, in a preliminary way, of a PV system, data (from the period 2007–2016 year retrieved from database [35]) regarding the solar radiations and

air temperatures for “Is Arenas” WWTP, Cagliari region, Italy, have been collected. Figure 3 shows the correlated data plotted by blue points highlighting the widespread trends and a high concentration from 300.0 W/m^2 for $15\text{--}25^\circ\text{C}$.

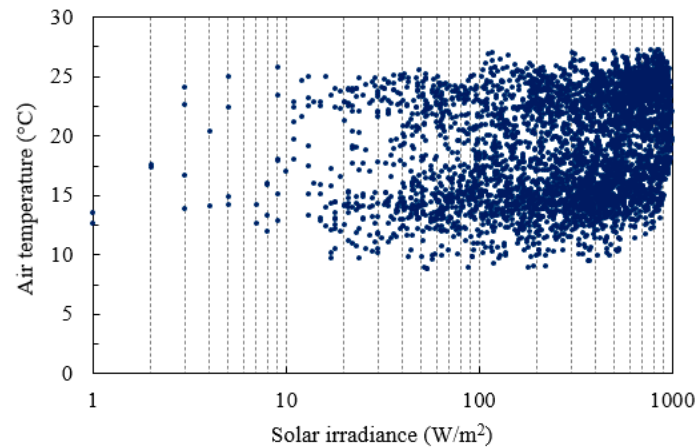


Figure 3. Solar irradiance/air temperature points at “Is Arenas” WWTP (Cagliari, Italy) [35].

Figure 4 shows the solar irradiance and air temperature curve during a day, indicating their possible correlation [15]. The air T curve could be consistent with the daily power outputs of a PVP: it assumes a null value between 7:00 p.m. and 4:00 a.m. and a very low value between 4 and 6 h and 17 and 19 h; therefore, in this example, only the values between 7 and 16 h have been considered.

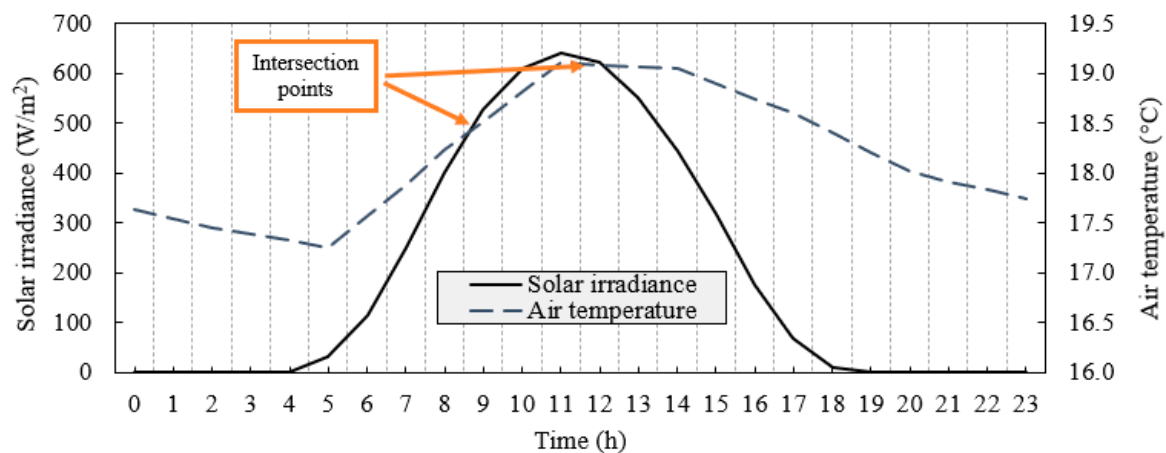


Figure 4. Solar irradiance/air temperature curves over time [35] (adapted from [12]).

By using the estimated global irradiances (Figure 3), a possible estimation of the produced mean energy for PVPs is defined. To verify the overlapping of the production of PV energy with the collected data due to the increasing of the energy consumption of aeration blowers, the following restraints were assumed: (i) the PV production during the months of a PVP has a peak power of 1 kWp; (ii) the energy consumption of WWTPs happen under the standard condition at 20°C , for the curve fluctuations of the air temperature during the months. Moreover, the used hypothesis is that, during the whole year, $R_{O_2} = 150 \text{ kg}_{R_{O_2}}/\text{month}$ (Equation (3)).

Table 2 lists the energy production of PVs by several parameters processed by database [35]. The peak value of the average daily sum of global irradiation received by the modules, $H(i)_d$, is $H(i)_d = 7.28 \text{ kWh/m}^2/\text{d}$, which is consistent with the literature’s [4] reference peak.

Table 2. PV energy production values processed by database [35].

| Month | E_d (kWh/d) | E_m (kWh/m) (Figures 5 and 6) | $H(i)_d$ (kWh/m ² /d) | $H(i)_m$ kWh/m ² /m) | $\pm\sigma_m$ (kWh) |
|---------------|---------------|------------------------------------|---------------------------------------|---------------------------------|---------------------|
| 1 (January) | 3.05 | 94.57 | 3.65 | 113.01 | 9.44 |
| 2 | 3.62 | 101.28 | 4.34 | 121.58 | 12.23 |
| 3 | 4.27 | 132.23 | 5.21 | 161.45 | 11.9 |
| 4 | 4.73 | 141.80 | 5.90 | 177.0 | 10.24 |
| 5 | 5.05 | 156.45 | 6.41 | 198.65 | 10.81 |
| 6 | 5.42 | 162.68 | 7.04 | 211.10 | 4.26 |
| 7 | 5.52 | 171.09 | 7.28 | 225.59 | 5.55 |
| 8 | 5.44 | 168.51 | 7.14 | 221.44 | 6.85 |
| 9 | 4.73 | 142.04 | 6.10 | 182.91 | 5.0 |
| 10 | 4.11 | 127.39 | 5.16 | 160.10 | 7.57 |
| 11 | 3.20 | 95.88 | 3.90 | 117.13 | 9.91 |
| 12 (December) | 2.89 | 89.50 | 3.47 | 107.48 | 9.46 |
| Mean | 4.34 | 131.95 | 5.47 | 166.45 | 2.40 |
| | | | | | |
| AOI loss (%) | | Spectral effects (%) | Temperature/solar irradiance loss (%) | Combined loss (%) | |
| −2.65 | | 0.66 | −5.93 | −20.73 | |

Note: E_d = Average daily energy production (kWh/d). E_m = Average monthly energy production (kWh/month). $H(i)_d$ = Average daily sum of global irradiation per square meter received by the modules (kWh/m²/d). $H(i)_m$ = Average monthly the solar irradiation sum per square meter received by the modules (kWh/m²/mm). σ_m = Standard deviation of the monthly energy production due to year-to-year variation (kWh). AOI = Angle of incidence.

Figure 5 shows the results in terms of the air temperature and PV energy production, E_m (Table 2), for each month. The air T curve considers the daily thermal variation; thus, it would measure only the seasonal trend (it refers to mean values for a period of 2007–2016 [35]).

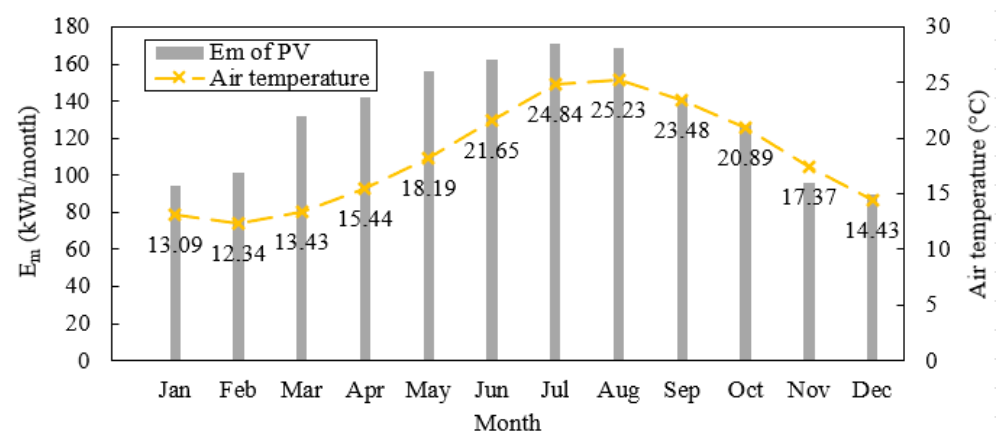


Figure 5. Air temperature curve and mean energy, E_m , of PV histograms [35] (adapted from [12]).

The results shown in Figure 2 should facilitate, in a parallel way, the design of PVPs with aeration systems to estimate a possible power value that optimizes the energy auto-consumption, improving future economic analyses for the investments of PVPs. The E_m histograms, shown in Figures 5 and 6, are proportional to the fluctuations of the air temperature during a season, where, as already mentioned, T is strongly correlated to the solar radiation curves in terms of amplitude and trend.

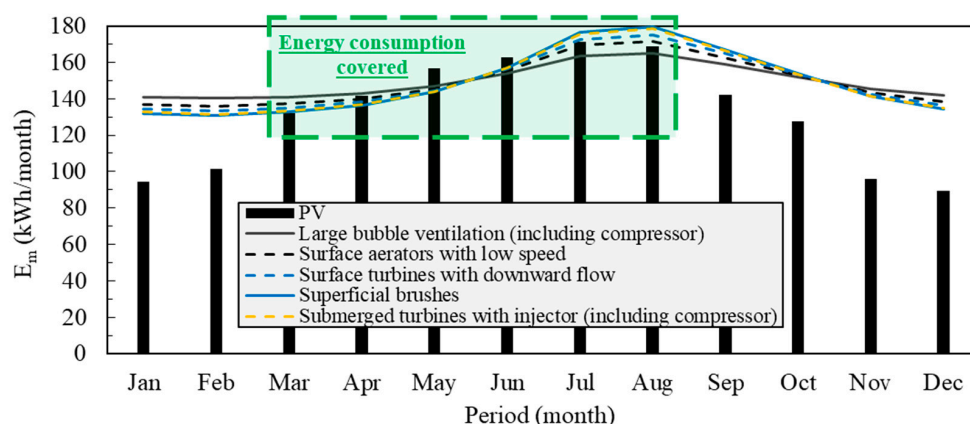


Figure 6. PV energy E_m and I_{pRO2} in WWTP for each aeration system.

By combining these E_m histograms with the I_{pRO2} curves (see Figure 2), plotted in function of the months, new results are obtained, as shown in Figure 6. In this way, the idea to correlate PVs to WWTPs is more evident, i.e., PV E_m histograms \leftrightarrow I_{pRO} curves.

The five curves in Figure 6 indicate a reduction in the energy consumption in the winter months and an increase in the summer months in the Mediterranean area (i.e., from June to August). Thus, if the blower's aeration system is known, it is possible to design an easy way to power the peak of PVPs that maximizes the annual auto-consumption of the oxidation tanks by using only the mean variation of the air temperature over a month. It is also possible to see that the energy consumption curves of the different aerator systems overlap in some points with a PV energy production of 1 kWp. These points indicate the optimum performance of the PV system.

Therefore, when E_m histograms of PV overlap the I_{pRO2} curves, the energy consumption is covered in an optimum way, for example, from March to August (see the green area in Figure 6). For the other cases, the performance is considered good (September–October) or poor (other months, not shown in Table 3). Finally, Table 3 shows the auto-consumption for the five blower systems.

Table 3. Auto-consumption for each aeration system (from March to October).

| Month | Auto-Consumption (%) for Aeration Systems | | | | | Performance |
|-------------------|---|-------------------------------------|----------------------------|--------------------------|----------------------------------|-------------|
| | Superficial Brushes | Surface Turbines with Downward Flow | Low-Speed Surface Aerators | Large Bubble Ventilation | Submerged Turbines with Injector | |
| 3 (March) | 100.0 | 98.0 | 96.0 | 94.0 | 99.0 | Optimum |
| 4 | 100.0 | 100.0 | 100.0 | 99.0 | 100.0 | |
| 5 | 100.0 | 100.0 | 100.0 | 100.0 | 100.0 | |
| 6 | 100.0 | 100.0 | 100.0 | 100.0 | 100.0 | |
| 7 | 97.0 | 99.0 | 100.0 | 100.0 | 97.0 | |
| 8 | 94.0 | 96.0 | 98.0 | 100.0 | 94.0 | Good |
| 9 | 85.0 | 86.0 | 87.0 | 89.0 | 85.0 | |
| 10 (October) | 83.0 | 83.0 | 83.0 | 84.0 | 83.0 | |
| Mean ^a | 87.0 | 87.0 | 87.0 | 86.0 | 87.0 | - |

^a The mean is calculated for the whole year (from January to December).

In Table 3, the mean auto-consumption in 1 year is $\geq 86.0\%$ for all systems, whereas the mean auto-consumption in the months ranges between 63.0% and 100.0% , with a spread of 8.0% (i.e., $\Delta I_{pRO2} = 18 - 10 = 8\%$ in August up to 14% by considering other aeration systems as shown in [13]), which should cover a part of 30.0% mentioned in Section 2.1.1.

Considering the energy production for PVs in a year, it is possible to conclude that in summer, spring, and in part of autumn (March to October), the mean auto-consumption

oscillates between 83.0% and 100.0%, whereas the mean auto-consumption in winter (from November to February, not shown in Table 3) reduces and oscillates between 63.0% and 77.0%.

4. Conclusions

This work presents a recent method proposed by authors to design PVs to optimize the energy auto-consumption of oxidation tanks in WWTPs. This method consists of providing, in a direct way, analytical equations to quantify the energy generation of PVs only using the air temperature, T , and the standard conditions of WWTPs. We conclude that:

(1) If the air temperature curve increases, the energy consumption in oxidation blowers also increase. Therefore, the designing of PVs should be carried out without a punctual measurement of the energy consumption of the oxidation tanks; however, just considering chemical parameters, e.g., biochemical oxygen demand, BOD_5 , volatile suspended solids, VSS, as there are easily recoverable in WWTPs. Thus, by considering the air temperature, the proposed equations should be excellent proxy functions for designing the necessary photovoltaic power and avoiding expensive energy and electric analyses in terms of time and analytical resolutions.

(2) The overlap of the energy consumption curves of the system and photovoltaic production curves should make the calculation of the power sufficient to individuate the maximize the energy auto-consumption. In this sense, the proposed approach would simplify the energy consumption analyses since traditional measurements used for controlling need available data (which, in many cases, can be difficult to retrieve) on WWTPs.

(3) The results show that the mean trend of Ip_{RO2} of the five aeration systems reaches a value of $\sim 8.0\%$ of the consumption of energy, with a temperature that varies between 20.0 and 25.0 °C. The consumption curves regarding the “superficial brushes” aeration system represent the technologies’ more energy intensiveness.

Author Contributions: Conceptualization, A.C.; methodology, A.C. and E.Z.; software, A.C.; validation, E.Z. and A.C.; formal analysis, A.C.; investigation, E.Z. and A.C.; data curation, A.C. and E.Z.; writing—original draft preparation, E.Z. and A.C.; writing—review and editing, E.Z. and A.C.; supervision, E.Z. and A.C. All authors have read and agreed to the published version of the manuscript.

Funding: This research received no external funding.

Institutional Review Board Statement: Not applicable.

Informed Consent Statement: Not applicable.

Data Availability Statement: Not applicable.

Acknowledgments: The first author thanks the Itecons institute, Coimbra, Portugal, and the University of Coimbra (UC), Portugal, to pay the rights (when applicable) to completely download all papers in the references.

Conflicts of Interest: The authors declare no conflict of interest.

References

1. Sharadga, H.; Hajimirza, S.; Balog, R.S. Time series forecasting of solar power generation for large-scale photovoltaic plants. *Renew. Energy* **2020**, *150*, 797–807. [\[CrossRef\]](#)
2. Nairn, C.; Rodriguez, I.; Segura, Y.; Molina, R.; Gonzalez-Benitez, N.; Molina, M.C.; Simarro, R.; Melero, J.A.; Martinez, F.; Puyol, D. Alkalinity, and not the oxidation state of the organic substrate, is the key factor in domestic wastewater treatment by mixed cultures of purple phototrophic bacteria. *Resources* **2020**, *9*, 88. [\[CrossRef\]](#)
3. Deep Purple Project. Available online: <https://deep-purple.eu/> (accessed on 1 June 2021).
4. Chakraborty, S. Reliable energy prediction method for grid connected photovoltaic power plants situated in hot and dry climatic condition. *SN Appl. Sci.* **2020**, *2*, 1–13. [\[CrossRef\]](#)
5. Sampaio, P.G.V.; Gonzalez, M.O.A. Photovoltaic solar energy: Conceptual framework. *Renew. Sustain. Energy Rev.* **2017**, *74*, 590–601. [\[CrossRef\]](#)

6. Serralta, J.; Ribes, J.; Seco, A.; Ferrer, J. A supervisory control system for optimising nitrogen removal and aeration energy consumption in wastewater treatment plants. *Water Sci. Technol.* **2002**, *45*, 309–316. [\[CrossRef\]](#)
7. Krzeminski, P.; Iglesias-Obelleiro, A.; Madebo, G.; Garrido, J.M.; van der Graaf, J.H.J.M.; van Lier, J.B. Impact of temperature on raw wastewater composition and active sludge filterability in full-scale MBR systems for municipal sewage treatment. *J. Membr. Sci.* **2012**, *423–424*, 348–361. [\[CrossRef\]](#)
8. Gallé, T.; Koehler, C.; Plattes, M.; Pittois, D.; Bayerle, M.; Carafa, R.; Christen, A.; Hansen, J. Large-scale determination of micropollutant elimination from municipal wastewater by passive sampling gives new insights in governing parameters and degradation patterns. *Water Res.* **2019**, *160*, 380–393. [\[CrossRef\]](#) [\[PubMed\]](#)
9. Rizzo, L.; Gernjak, W.; Krzeminski, P.; Malato, S.; Mc Ardell, C.S.; Sanchez Perez, J.A.; Schaar, H.; Fatta-Kassinos, D. Best available technologies and treatment trains to address current challenges in urban wastewater reuse for irrigation of crops in EU countries. *Sci. Total Environ.* **2020**, *710*, 1–17. [\[CrossRef\]](#)
10. Khan, S.A.R.; Ponce, P.; Yu, Z.; Golpira, H.; Mathew, M. Environmental technology and wastewater treatment: Strategies to achieve environmental sustainability. *Chemosphere* **2022**, *286*, 1–10. [\[CrossRef\]](#) [\[PubMed\]](#)
11. Strazzabosco, A.; Kenway, S.J.; Lant, P.A. Quantification of renewable electricity generation in the Australian water industry. *J. Clean. Prod.* **2020**, *254*, 120119. [\[CrossRef\]](#)
12. Colacicco, A.; Zacchei, E. Optimization of energy consumptions of oxidation tanks in urban wastewater treatment plants with solar photovoltaic systems. *J. Environ. Manag.* **2020**, *276*, 111353. [\[CrossRef\]](#)
13. Alvarez-Guerra, E.; Dominguez-Ramos, A.; Irabien, A. Photovoltaic solar electro-oxidation (PSEO) process for wastewater treatment. *Chem. Eng. J.* **2011**, *170*, 7–13. [\[CrossRef\]](#)
14. Rosa-Clot, M.; Tina, G.M.; Nizetic, S. Floating photovoltaic plants and wastewater basins: An Australian project. *Energy Procedia* **2017**, *134*, 664–674. [\[CrossRef\]](#)
15. Wu, W.; Christiana, V.I.; Chen, S.A.; Hwang, J.J. Design and techno-economic optimization of a stand-alone PV (photovoltaic)/FC (fuel cell)/battery hybrid power system connected to a wastewater-to-hydrogen processor. *Energy* **2015**, *84*, 462–472. [\[CrossRef\]](#)
16. Ganiyu, S.O.; Brito, L.R.D.; da Araújo Costa, E.C.T.; dos Santos, E.V.; Martínez-Huitle, C.A. Solar photovoltaic-battery system as a green energy for driven electrochemical wastewater treatment technologies: Application to elimination of brilliant blue FCF dye solution. *J. Environ. Chem. Eng.* **2019**, *7*, 102924. [\[CrossRef\]](#)
17. Valero, D.; Ortiz, J.M.; Exposito, E.; Montiel, V.; Aldaz, A. Electrochemical wastewater treatment directly powered by photovoltaic panels: Electrooxidation of a dye-containing wastewater. *Environ. Sci. Technol.* **2010**, *44*, 5182–5187. [\[CrossRef\]](#) [\[PubMed\]](#)
18. Strazzabosco, A.; Kenway, S.J.; Lant, P.A. Solar PV adoption in wastewater treatment plants: A review of practice in California. *J. Environ. Manag.* **2019**, *248*, 109337. [\[CrossRef\]](#)
19. Andrei, H.; Badea, C.A.; Andrei, P.; Spertino, F. Energetic-environmental-economic feasibility and impact assessment of grid-connected photovoltaic system in wastewater treatment plant: Case study. *Energies* **2021**, *14*, 100. [\[CrossRef\]](#)
20. Mou, Y.; Xia, Y.; Zhang, S.; He, Y.; Shen, W.; Li, J. Aniline removed from simulated wastewater by electro-Fenton process using electric energy from photovoltaic modules. *Desalination Water Treat.* **2022**, *247*, 173–183. [\[CrossRef\]](#)
21. Marmanis, D.; Emmanouil, C.; Fantidis, J.G.; Thysiadou, A.; Marmani, K. Description of a Fe/Al electrocoagulation method powered by a photovoltaic system, for the (ore-)treatment of municipal wastewater of a small community in Northern Greece. *Sustainability* **2022**, *14*, 4323. [\[CrossRef\]](#)
22. Clerici, A. Efficienza energetica nel settore idrico. In Proceedings of the Efficienza Energetica—Tutela Dell’Ambiente, Opportunità di Crescita, Technical Workshop, Milan, Italy, 12 September 2011.
23. Vaccari, M. Il consumo energetico negli impianti di depurazione. In Proceedings of the Il Consumo di Energia Elettrica Negli Impianti di Depurazione: Opportunità di Risparmio, Meeting, Rimini, Italy, 8 November 2012.
24. Di Domenico, S. Analisi Delle Fognature e Relative Applicazioni Energetiche. Bachelor Dissertation, University of Bologna, Bologna, Italy, 2010; p. 176.
25. United Nations (UN). *Transforming Our World: The 2030 Agenda for Sustainable Development*; Technical Report A/RES/70/1; United Nations (UN): New York, NY, USA, 2015; p. 35.
26. Directive 2000/60/EC, European Parliament and of the Council, A Framework for Community Action in the Field of Water Policy, OJ L 327, 22.12.2000, p. 73. 2000. Available online: <https://eur-lex.europa.eu/legal-content/EN/TXT/?uri=CELEX%3A32000L0060> (accessed on 1 August 2020).
27. Zhang, H.; Gong, W.; Bai, L.; Chen, R.; Zeng, W.; Yan, Z.; Li, G.; Liang, H. Aeration-induced CO₂ stripping, instead of high dissolved oxygen, have a negative impact on algae-bacteria symbiosis (ABS) system stability and wastewater treatment efficiency. *Chem. Eng. J.* **2020**, *382*, 122957. [\[CrossRef\]](#)
28. Liu, G.; Wang, J.; Campbell, K. Formation of filamentous microorganisms impedes oxygen transfer and decreases aeration efficiency for wastewater treatment. *J. Clean. Prod.* **2018**, *189*, 502–509. [\[CrossRef\]](#)
29. Pennsylvania Department of Environmental Protection. *The Activated Sludge Process, Part II, Module 16, Wastewater Treatment Plant, Operator, Certification Training*; Pennsylvania Department of Environmental Protection: Harrisburg, PA, USA, 2014; p. 114.
30. Capuano, M. Modello di Calcolo Diagnostico del Comparto di Aerazione in un Impianto di Depurazione Delle Acque Reflue Civili a Scala Reale. Master’s Dissertation, Polytechnic of Torino, Torino, Italy, 2018; p. 164.
31. Gillot, S.; Héduit, A. Effect of air flow rate on oxygen transfer in an oxidation ditch equipped with fine bubble diffusers and slow speed mixers. *Water Res.* **2000**, *34*, 1756–1762. [\[CrossRef\]](#)

-
32. Lu, J.H.; Lei, H.Y.; Dai, C.S. Analysis of Henry's law and a unified lattice Boltzmann equation for conjugate mass transfer problem. *Chem. Eng. Sci.* **2019**, *199*, 319–331. [[CrossRef](#)]
 33. Mizuta, K.; Shimada, M. Benchmarking energy consumption in municipal wastewater treatment plants in Japan. *Water Sci. Technol.* **2010**, *62*, 2256–2262. [[CrossRef](#)] [[PubMed](#)]
 34. Campanelli, M.; Foladori, P.; Vaccari, M. *Consumi Elettrici ed Efficienza Energetica del Trattamento Delle Acque Reflue*; Maggioli Editore: Santarcangelo di Romagna, Italy, 2013; p. 391.
 35. PVGIS. Photovoltaic Geographical Information System. Database. 2020. Available online: <https://ec.europa.eu/jrc/en/pvgis> (accessed on 1 January 2020).